On the Impact of Radio Propagation Models on MANET Simulation Results

Illya Stepanov, Daniel Herrscher, Kurt Rothermel

Institute of Parallel and Distributed Systems (IPVS)
Universität Stuttgart
Universitätsstr. 38
70569 Stuttgart, Germany
{stepanov, herrscher, rothermel}@informatik.uni-stuttgart.de

Contact details of the first author:

Illya Stepanov
Institute of Parallel and Distributed Systems (IPVS)
Universität Stuttgart
Universitätsstr. 38
70569 Stuttgart, Germany

Tel.: +49/711/7816-442
Fax: +49/711/7816-424
Email: stepanov@informatik.uni-stuttgart.de

Abstract: Network simulation tools are frequently used to analyze performance of MANET protocols and applications. They commonly offer only simple radio propagation models that neglect obstacles of a propagation environment. In this paper, we integrate a more accurate radio propagation model into a simulation tool. The model is based on ray tracing and considers geographic data of the simulation area. We prove that the usage of a more precise propagation model changes simulated connection topologies considerably. Consequently, we obtain different performance evaluation results. To our best knowledge, no other study of MANETs has been performed so far with such a detailed radio propagation model. Hence, this paper also gives new insights on the realistic performance of MANETs in outdoor environments.

Index terms: Communication systems, mobile communication, UHF propagation, geographic information systems, simulation

On the Impact of Radio Propagation Models on MANET Simulation Results

Illya Stepanov, Daniel Herrscher, Kurt Rothermel
Institute of Parallel and Distributed Systems (IPVS), Universität Stuttgart
Universitätsstr. 38
70569 Stuttgart, Germany
{stepanov, herrscher, rothermel}@informatik.uni-stuttgart.de

Abstract — **Network simulation tools are frequently used to analyze performance of MANET protocols and applications. They commonly offer only simple radio propagation models that neglect obstacles of a propagation environment. In this paper, we integrate a more accurate radio propagation model into a simulation tool. The model is based on ray tracing and considers geographic data of the simulation area. We prove that the usage of a more precise propagation model changes simulated connection topologies considerably. Consequently, we obtain different performance evaluation results. To our best knowledge, no other study of MANETs has been performed so far with such a detailed radio propagation model. Hence, this paper also gives new insights on the realistic performance of MANETs in outdoor environments.**

Index Terms — **Communication systems, mobile communication, UHF propagation, geographic information systems, simulation**

I. Introduction

Mobile ad-hoc networks (MANETs) are created spontaneously by wireless communication peers, without relying on a fixed infrastructure. The devices communicate directly with each other when they are in transmission range. Common communication technologies are Bluetooth [17] and IEEE 802.11 [19]. Special ad-hoc routing algorithms are used for multi-hop communication.

Network simulation tools [2], [8], [16] are frequently used to analyze the performance of MANET protocols and applications. These tools model the applications running on mobile devices, the wireless network protocol stack, radio signal propagation, and the mobility of the network users.

The radio propagation models used in common MANET simulators assume an obstacle-free area and a free line-of-sight between all communicating partners. As a consequence, the communication range is modeled by a simple circle around the mobile device. However, this poorly reflects radio wave propagation in a typical outdoor scenario, like a city center, in which buildings significantly affect the communication between nodes. Nevertheless, the vast majority of publications that investigate MANET protocol and application behavior still relies on such simple models.

In this paper, we integrate a more accurate radio propagation model into ns-2 [2], which is the most widely used network simulator. The model is based on ray tracing and considers geographic data of the simulation area, which are available from digital map vendors. We use an existing implementation of the propagation model from a specialized tool for network planning [1]. We prove that the usage of a more precise radio propagation model changes simulation results considerably. In our sample simulations, we consider both the network connectivity and the performance of network applications. To our best knowledge, no other study of MANETs has been performed so far with such a detailed radio propagation model. Hence, this paper also gives new insights on the performance of MANETs in outdoor environments.

The remainder of this paper is structured as follows. In Section II, we describe the radio propagation models we used and their integration to ns-2. In Section III, we present our scenario and simulation results. Section IV gives an overview of related work. Section V concludes this paper.

II. Radio Propagation Models and their Integration to ns-2

In the following, we consider ns-2 as MANET simulation tool [2], because it is adopted widely in the community. However, our general considerations are valid for most other tools as well.

Each time a mobile node transmits a frame in a simulation, ns-2 uses a propagation model to calculate the receive power of the radio signal for every potential receiving node. Similar to real world, the frame is received correctly if the corresponding signal strength is not below the receive threshold of the network equipment (*RXThresh*). If the receive signal strength is below the receive threshold but it is above or equals the carrier-sense threshold (*CSThresh*), the frame is received with errors. Another frame arriving at the same time causes a collision if its signal power is not at least collision threshold (*CPThresh*) times below this frame's signal strength. All frames with a power below the carrier sense threshold are ignored by the receiver.

Hence, the radio propagation model is the key factor to determine which nodes can communicate. It also influences frame collisions and errors in a simulation. Obviously, to get

realistic simulation results, it is essential to use a realistic radio propagation model.

A. Radio Propagation Models for Outdoor Scenarios

We consider radio propagation models for ultra-high frequency (UHF) communication technologies in outdoor environments. They can be classified into two major groups: empirical models and ray optical models. Empirical models come as formulas that provide estimations for the receive power based on the distance between the communication partners. Ray optical models use ray tracing or similar techniques to determine possible signal paths between the transmitter and the receiver in the given area. In this section, we first briefly describe two empirical models, which are already integrated in ns-2 and therefore are commonly used in MANET simulations. Then, we present the "intelligent ray tracing" model, which provides more realistic results.

1) Combination of Free Space and Two-Ray Ground Models

The "free space" model was proposed by Friis [6]. It assumes exactly one path between the transmitter and the receiver. The path must be clear from obstacles.

$$P_r = \frac{P_t G_t G_r \lambda^2}{(4\pi)^2 d^2 L} \quad (1)$$

where: P_r is the received signal power (in W), P_t is the transmitted signal power, G_r and G_t are the gains of the receiving and the transmitting antennas respectively, λ is the wave length, L is the system loss, and d is the distance between the transmitter and the receiver.

According to [7], a single direct path between the communicating partners exists seldom at larger distances. The "two-ray ground" model considers both the clear path and the ground reflected path:

$$P_r = P_t G_t G_r \frac{h_t^2 h_r^2}{d^4 L} \quad (2)$$

In addition to the parameters of the free space model, the equation contains h_r and h_t, which are the heights of receiving and the transmitting antennas respectively. Similar to the free space model, the model neglects obstacles of the propagation environment.

However, the two ray ground model is too optimistic for the short transmitter-receiver separation distances. Hence, in most applications, the two models are combined. The free space model is used at small distances, while the two-ray ground model is used at larger distances. The distance at which both models give identical results ($d_c = 4\pi h_t h_r / \lambda$) is used as cross-over distance. In our paper, we use the combination of these two models as a reference model.

2) Log-Distance Path-Loss Model

This model expresses the decrease of the received power with distance raised to some exponent:

$$P_r = P_{r0}\left(\frac{d_0}{d}\right)^{\beta} \quad (3)$$

where: P_{r0} is the free space receive power at the close-in reference distance d_0, β is the path-loss exponent. Usually $d_0 = 1\ m$.

The exponent β depends on the propagation environment. For the open-space area like in the free space model, $\beta = 2$. For urban areas with obstacles, β is between 2.5 and 3.5. Manufactures of wireless cards normally use $\beta = 2.7$ to specify the maximum transmission range for a typical outdoor environment (cp. [13]). In our paper, we use the log-distance path-loss model with $\beta = 2.5, 2.7, 3.0, 3.5$ as another reference model.

3) Intelligent Ray Tracing Model

The main advantage of the empirical models described above lies in their simplicity and therefore in their low computational complexity. However, since the distance between the sender and the receiver is the only dynamic parameter of these models, the communication area defined by $P_r \geq RXThresh$ is simply a circle. The models do not take the geographic environment into account. As depicted in Figure 1, this poorly reflects the reality in urban environments.

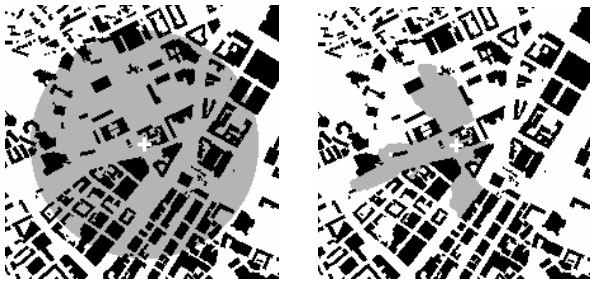

Figure 1: Communication area of a WLAN node computed with the combined two-ray ground model (on the left) and the ray tracing model (on the right). The transmitter is partially blocked by buildings.

Ray optical models use ray tracing to determine all possible signal paths between the transmitter and the receiver. They consider a geographic map of the simulation area. Reflection, diffraction, and scattering of radio waves are taken into account. The components of individual paths are summed to obtain the receive signal power. The models provide accurate results, but require longer computation time.

In this paper, we use the "intelligent ray tracing" model [20], which is an improved version of the classic ray tracing approach. In order to accelerate the performance of ray tracing, the model preprocesses the digital map and computes visibility relations between walls, thus achieving the acceleration factor near 1000. The accuracy of the model is proven by measurements in European cities [11], [15].

B. Implementation

The simulation tool ns-2, which we use for our integration and sample measurements, already provides the combination of the free space and the two-ray ground models (called "two-ray ground model" for simplicity) and the log-distance path-loss model (called "shadowing model"). In the following, we describe how we integrate the intelligent ray tracing model to ns-2.

We use a commercial implementation of the intelligent ray tracing model (WinPROP by AWE Communications [1]). As input, WinPROP requires a 2.5-dimensional geographic model of the target area. We extracted the necessary data from the digital map of Stuttgart city center (the whole area size is about 2.4 km × 1.9 km). For any given sender position (and other static parameters like sender height, transmission power, wavelength etc.), WinPROP can calculate a map of receive power values for a grid, representing possible positions of a receiver. The algorithm implemented in WinPROP does not allow to calculate the receive power for just one receiver position efficiently. In our simulations, we use a 5 m × 5 m grid, which is the smallest grid size we could handle. We performed a separate investigation to assure that the chosen grid size has minor impact on simulation results.

Because it takes WinPROP about 30 s to calculate a receive power map for one sender position, it would not be sensible to call WinPROP every time ns-2 needs a receive power value; this would lead to several million calls for one simulation. Instead, we precalculated the receive power values for each possible sender-receiver pair in our scenario in a 5 m × 5 m grid. For our scenario size, this translates to about 32 billions of position pairs. The precalculation step took three days on a 50-node PC cluster and produced about 120 GB of output data (since we store each value in a 4-byte float).

To use the calculated data with ns-2, we implemented our own radio propagation module. Each time ns-2 needs a receive power value, our module reads the appropriate value from the dataset. To reduce the data access overhead, our module implements a caching strategy. As the result, the overall ns-2 simulation time with our propagation module is comparable to the simulation time using a traditional, empirical model.

III. Simulations

A. Scenario

To investigate the impact of different radio propagation models on MANET simulation results, we use a typical simulation scenario (Table 1). A MANET is formed by 100 mobile users in a city center. We consider the Stuttgart city center as simulation area. For the modeling of user mobility, we use the "user-oriented mobility model" described in [18]. We generated randomly user trips in the simulation area. The movement area is constrained to the dense street network of Stuttgart downtown (1.5 km × 1.5 km). The coordinates of streets are taken from the same digital map as the building information. The movement paths between trip points are calculated with the Dijkstra shortest-path algorithm [5]. Users move with a speed chosen randomly between 2 and 5 km/h.

In our scenario, the users are equipped with mobile devices. The devices communicate wirelessly using IEEE 802.11b. We take the basic hardware parameters (transmission power and receive threshold) from hardware datasheets [13]. The carrier-sense threshold and the collision threshold, which are not directly specified by hardware manufacturers, are set to the values suggested in [21].

In our sample simulations, we use the following radio propagation models: the two-ray ground model, the log-distance path-loss model with β=2.5, 2.7, 3.0, 3.5, and the intelligent ray-tracing model.

To compare routing protocol performance, we simulate constant-bit rate traffic between some users (5 connections between 8 users). For multi-hop routing, we use ad-hoc on-demand distance vector routing (AODV) [14].

Table 1: Parameters of the simulation scenario

Simulation time	900 s
Transmission power (P_t)	15 dBm
Radio frequency	2.442 GHz
Transmission speed	1, 2, 5.5, 11 Mbps
Receive threshold (*RXThresh*)	-94, -91, -87, -82 dBm (depending on transmission speed)
Carrier-sense threshold (*CSThresh*)	-104 dBm
Collision threshold (*CPThresh*)	10 dB
System loss (L)	1
Antenna type	Omnidirectional
Antenna gain (G)	1
Antenna height (h)	1.5 m
Data traffic	Constant-bit rate traffic
Packet size	512 bytes
Data traffic intensity	1 packet/s

B. Comparison of MANET Topologies

First, we demonstrate the impact of radio propagation models on MANET connectivity. To monitor the change in topologies in time, we use a custom event-based topology simulation tool in addition to ns-2. The tool determines for every pair of mobile nodes times when they enter or leave each other's transmission range. Thereby we construct MANET topology graphs at different time steps.

1) Metrics

For the comparison, we use the following metrics.

Number of edges in the MANET topology graph

corresponds to the total number of direct connections between nodes. We consider that a node j is connected to a node i if it receives transmissions from i with the signal power above the receive threshold. The maximum number of edges in our scenario is $N \times N$, where N is the number of nodes in the network: $100 \times 100 = 10{,}000$.

We use the *hamming distance* to express difference between two topology graphs. We represent a graph with the adjacency matrix $T(x_{ij})$, $i=1 .. N$, $j=1 .. N$, where, x_{ij} is a bit value of 1 if the edge $i \rightarrow j$ exists, and 0 otherwise. Then the hamming distance between two matrices is the number of elements that the matrices differ on. Since we consider the edge $i \rightarrow i$ exists always (since we use omnidirectional antennas), the maximum hamming distance for topologies in our scenario is 9,900, which corresponds to the case that two graphs have only $i \rightarrow i$ connections in common.

In the charts, we present the *weighted average* of results. So, we aggregate individual results by taking into account the relevance of each component, which is the duration of time that the network connectivity graph was in the particular state.

2) Results

In Figure 2, we compare the average number of edges in MANET graphs for different transmission speeds with different radio propagation models.

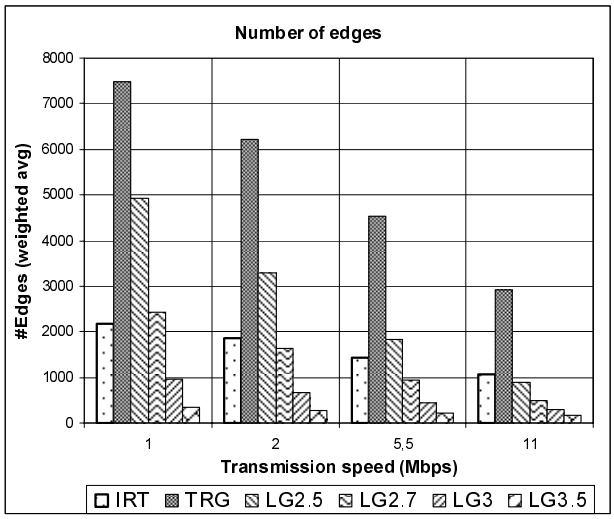

Figure 2: Average number of edges in topologies

Clearly, since the communication according to the two-ray ground model (TRG) is possible at very long distances (e.g., up to 796 m at 1 Mbps according to equation 1), the result graphs are tightly connected. They contain a large number of edges (e.g., more than 70% of all possible edges at 1 Mbps). As we see further, this increases a chance of network collisions. In contrast, the log-distance path-loss model with $\beta=3.5$ (LG3.5) produces too pessimistic results. LG2.7 at 1 and 2 Mbps, LG2.5 at 5.5 and 11 Mbps seem to resemble the intelligent-ray tracing (IRT) model at closest.

However, the hamming distance (Figure 3) shows significant difference in graphs. For example, at 1 Mbps, the topologies of LG2.7 and IRT differ on average at 1470 edges. By taking into account that the topologies consist on average of 2420 and 2190 edges respectively (Figure 2), they differ in more than 50% of edges.

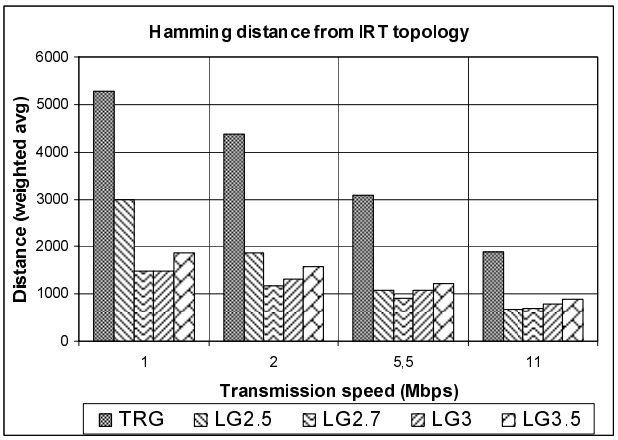

Figure 3: Hamming distance from the topology with the intelligent ray tracing model

The hamming distance between two topology graphs corresponds to the number of the edges that exist only in one topology. Figure 4 and Figure 5 show where the difference comes from.

a) Some edges are missing in IRT. Such edges are blocked by communication obstructions. These edges constitute the main difference for the models that have relatively long transmission ranges, like TRG.

b) Some edges exist only in IRT and are missing in LG topologies. As shown in Figure 1, IRT and TRG have equal transmission range in a free space area. By applying the LG model with β greater than 2, we decrease transmission range

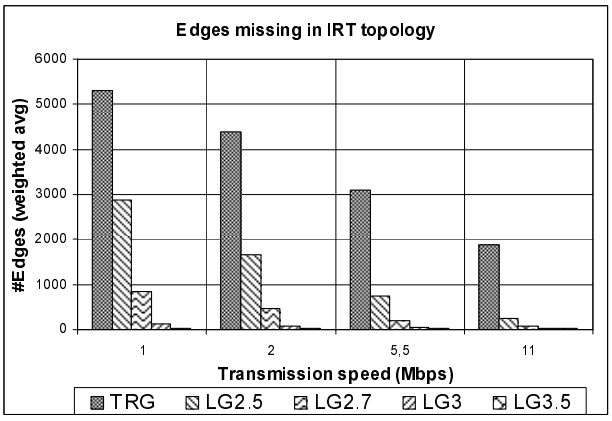

Figure 4: Average number of edges missing with the intelligent ray tracing model

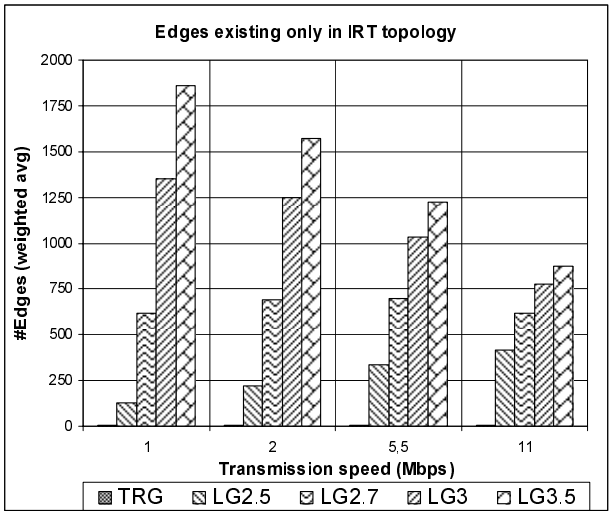

Figure 5: Average number of edges existing only with the intelligent ray tracing model

in order to reflect the propagation in obstructed areas. However, we then underestimate propagation in open areas.

A separate study (we do not present the corresponding charts due to space limitation) showed that TRG topologies at all transmission speeds, LG2.5 at 1 and 2 Mbps, LG2.7 at 1 Mbps are fully connected. With these models, we expect that the routing protocol delivers nearly 100% of data packets. LG3.5 topology at all transmission speeds, LG3.0 at 5.5 and 11 Mbps, and LG2.7 at 11 Mbps are heavily partitioned. We expect relatively small percentage of data packets being delivered with these models. On average, in IRT topology at all transmission speeds more than 90% of all nodes are in the same partition.

The results presented in this section prove that the application of the more accurate radio propagation model considerably changes topologies in a MANET simulation. In the next section, we investigate the impact of radio propagation models on MANET application performance.

C. *Analysis of Routing Protocol Performance*

1) *Metrics*

Data packet delivery ratio is the ratio between the number of data packets successfully delivered to recipients and the number of data packets originated by constant-bit rate (CBR) sources.

Routing packet overhead is the ratio between the number of routing packets and the total number of packets sent.

Data packet delay is the time elapsed from the data packet origination at a source and its delivery to the recipient. *Hop count* is the number of nodes that a data packet traversed to the recipient. It is important to note that these two metrics consider only the packets successfully delivered to recipients.

In the charts below, we present the *geometric average* of results obtained with 20 simulation runs with different randomly generated mobility patterns.

2) *Results*

Figure 6 shows the data packet delivery ratio. As we expected from the analysis of network partitioning, there are very few packets delivered in the simulations with LG3.5 at all transmission speeds, LG3.0 at 5.5 and 11 Mbps, and LG2.7 at 11 Mbps. The results of LG3.0 at 1 Mbps, TRG at 2 Mbps, LG2.7 at 5.5 Mbps, and LG2.5 at 11 Mbps seem to be close to IRT, which are above 80% at 5.5 and 11 Mbps and are above 90% at other transmission speeds. It is notable that in the simulations with TRG at 1 and 2 Mbps we unexpectedly see fewer packets delivered in comparison to other radio propagation models. The reason is that AODV uses flooding to find a route to the destination. In densely connected networks formed with the TRG model, this leads to frequent packet collisions when multiple nodes initiate route discoveries. The collisions stress both route discoveries and data packet transmissions. Figure 7, which presents the results of routing packet overhead, proves these assumptions.

According to Figure 7, about 65% of routing packets are sent in the simulations with IRT model at all transmission speeds. For other models except TRG at 1 and 2 Mbps, the higher is the transmission speed, the more routing packets are sent. The same is observable for LG model with the increase of path-loss exponent β. This occurs because at higher transmission speeds or with larger β the network becomes less connected and more routing packets are required for route search and maintenance.

Figure 8 shows the average path lengths. Obviously, because of the observed network connectivity, the shorter paths are in simulations with TRG. For LG model, the path lengths increase with the increase of path-loss exponent, since in a less connected network more hops need to be traversed to a destination. It is necessary to admit that the results for

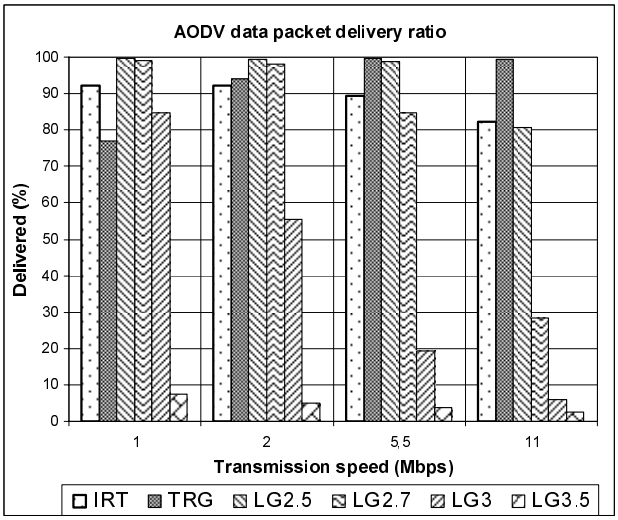

Figure 6: AODV data packet delivery ratio

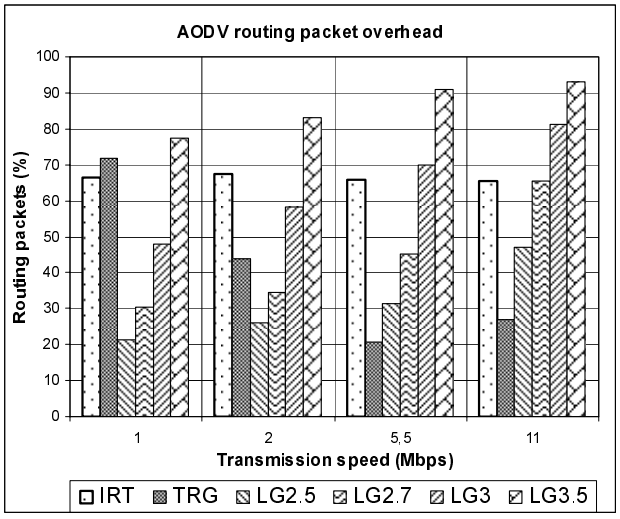

Figure 7: AODV routing packet overhead

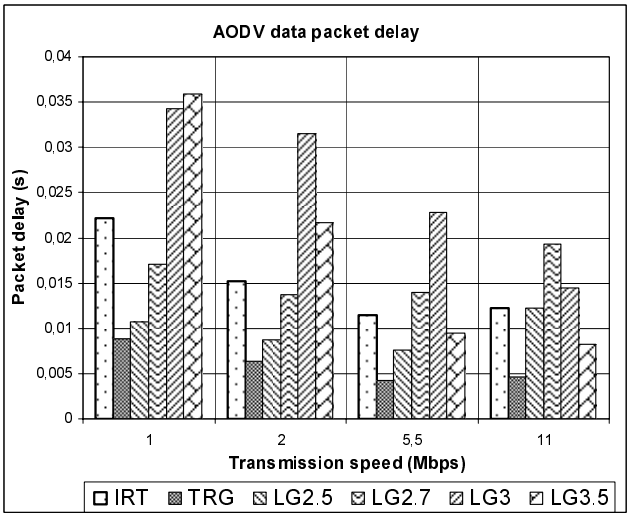

Figure 9: AODV data packet delay

LG3.5 at all transmission speeds, LG3.0 at 5.5 and 11 Mbps, and LG2.7 at 11 Mbps are not representative, since we consider only few samples due to low packet delivery ratio. The path lengths in IRT simulations at 1 Mbps are similar to those for LG2.7. At 2 Mbps, the IRT results are between LG2.5 and LG2.7. At 5.5 Mbps, they are similar to LG2.5. At 11 Mbps, the IRT results are between TRG and LG2.5.

Figure 9 shows the average data packet delay observed in our simulations. At the same transmission speed, the shortest data packet delay is in the simulations with TRG model. For LG model, the delay increases with the increase of path-loss exponent. That happens because the network becomes less connected, so more time is required for route discovery. Also the paths become longer. The results for LG3.5 at 2, 5.5, and 11 Mbps, LG3.0 at 11 Mbps are not representative, since we count too few samples due to low packet delivery ratio. The packet delay in simulations with IRT at 1 and 2 Mbps is between the results of LG2.7 and LG3.0. At 5.5 Mbps, the IRT results are between the results of LG2.5 and LG2.7. At 11 Mbps, the IRT results are similar to LG2.5.

For the same radio propagation model, the delay decreases with the increase of transmission speed from 1 to 5.5 Mbps. However, the delay starts to increase at 5.5 Mbps for LG2.7 and at 11 Mbps for other models. Here, route discovery and maintenance in a less-connected network takes more time that what is gained by a faster transmission speed.

From the analysis, we see that due to significant changes in simulated network topologies, the IRT model produces different results compared to the empirical models commonly used in ns-2. In our scenario, the results for data packet delivery ratio, end-to-end delays and path lengths in simulations with IRT model are similar to the results of log-distance path-loss model with rather low β (2.5 .. 2.7). However, we see much higher routing overhead, which is similar to the overhead for log-distance path-loss model with rather high β (3.0 .. 3.5). Hence, we see that a more accurate radio propagation model cannot simply be replaced by an empirical model with special parameter settings.

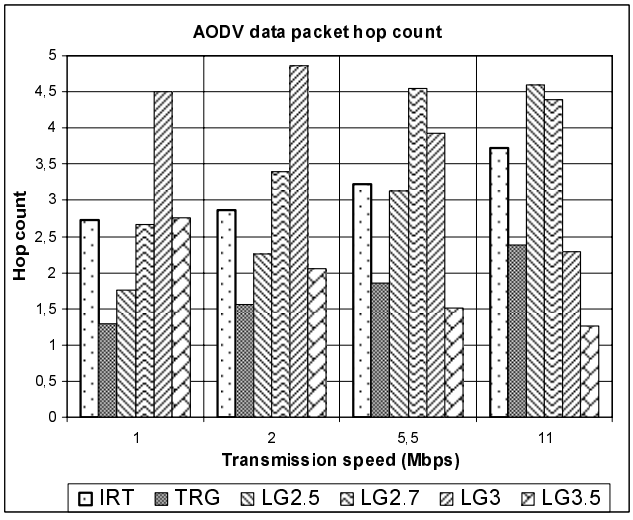

Figure 8: AODV data packet hop count

IV. Related Work

A detailed statistics about the publications at top MANET conferences in [12] proves that the papers with simple radio propagation models outnumber others significantly. Most authors are only interested in a comparative performance analysis of their protocols and applications, like in [3]. For their studies, they use open-space areas without obstacles.

The widely used MANET simulation tools ns-2 [2], GloMoSim [8], and GTNetS [16] offer only the free space model and the two-ray ground model. In addition, ns-2 provides the shadowing model, which is basically the log-distance path-loss model extended with a random term.

In [10], the authors consider communication obstructions of a simulation area. They assume a communication between two nodes is not possible if a direct path between them is blocked with an obstacle. The authors agree that this approach is a too simple workaround, since it neglects multipath propagation of radio waves.

In [9], the authors make a step towards improving the radio propagation modeling for MANET simulations. They integrate the empirical COST-Walfisch-Ikegami model [4] into ns-2 simulation environment. Besides other parameters of empirical radio propagation models, this model considers the heights of the transmitter and the receiver, mean building height, mean width of roads, mean building separation, and road orientation with respect to the direct radio path. Clearly, the Walfisch-Ikegami model is more realistic than other empirical models that do not consider geographic information at all. However, ray tracing models are much more realistic as they also reflect the propagation paths in the horizontal plane.

V. Conclusion

In this paper, we showed how to integrate a ray tracing model for wave propagation into ns-2. The model accurately reflects radio propagation in outdoor scenarios, which has been proven by measurements in European cities [11], [15]. We demonstrated that the usage of more accurate radio propagation model changes simulated topologies considerably compared to commonly used propagation models. Consequently, we obtain different performance evaluation results.

Obviously, there are many scenarios in which application of such a complex propagation model is unnecessary. For example, an open space area with the two-ray ground model might be sufficient for comparing two routing protocols. However, researchers must be aware of significant difference between the real connection topologies and the topologies obtained with simple models offered by MANET simulation tools. For obtaining quantitative performance evaluation results in the target area, more accurate radio propagation models need to be used. As we showed in this paper, it is possible to integrate these models into ns-2.

VI. Acknowledgment

We thank Philipp Wertz (Institute of Radio Frequency Technology, Universität Stuttgart) and Hermann Buddendick (AWE Communications) for their support regarding the radio propagation software. We also thank Jan Geiger, Jörg Hähner, and Abdelmajid Khelil for their valuable comments on the paper.

References

[1] AWE Communications Home Page. Available at http://www.awe-communications.com

[2] L. Breslau, D. Estrin, K. Fall, S. Floyd, J. Heidemann, A. Helmy, P. Huang, S. McCanne, K. Varadhan, Y. Xu, and H. Yu, "Advances in Network Simulation," *IEEE Computer*, Vol. 33, No. 5, May 2000.

[3] J. Broch, D. Maltz, D. Johnson, Y. Hu and J. Jetcheva, "A Performance Comparison of Multi-Hop Wireless Ad Hoc Network Routing Protocols," in *Proceedings of the 4th Annual ACM/IEEE International Conference on Mobile Computing and Networking (MobiCom'98)*, Dallas, USA, October 1998.

[4] COST-231, "Urban transmission loss models for mobile radio in the 900- and 1800 MHz bands," Revision 2, September 1991.

[5] E. W. Dijkstra, "A note on two problems in connection with graphs," *Numerische Mathematik*, 1, pp. 269–271, 1959.

[6] H. T. Friis, "A note on a simple transmission formula," in *Proceedings of IRE*, Vol. 41, 1946.

[7] J. D. Gibson, *The Communications Handbook*, CRC Press, ISBN: 0849383498, 1997.

[8] GloMoSim: Global Mobile Information Systems Simulation Library. Available at http://pcl.cs.ucla.edu/projects/glomosim

[9] I. Gruber, O. Knauf, H. Li, "Performance of Ad Hoc Routing Protocols in Urban Environments,", in *Proceedings of European Wireless 2004 (EW'2004)*, Barcelona, Spain, February 2004.

[10] P. Johansson, T. Larsson, N. Hedman, B. Mielczarek, and M. Degermark, "Scenario-based performance analysis of routing protocols for mobile ad-hoc networks," in *Proceedings of the 5th ACM/IEEE International Conference on Mobile Computing and Networking (MobiCom'99)*, Seattle, USA, August 1999.

[11] R. Hoppe, G. Wölfle, and F. M. Landstorfer, "Fast 3D Ray Tracing for the Planning of Microcells by Intelligent Preprocessing of the Database," in *Proceedings of the 3rd European Personal and Mobile Communications Conference (EPMCC) 1999*, Paris, France, March 1999.

[12] D. Kotz, C. Newport, R. S. Gray, J. Liu, Y. Yuan, and C. Elliott, "Experimental evaluation of wireless simulation assumptions," Dartmouth Computer Science Technical Report TR2004-507, June 2004.

[13] *Orinoco® 11b Client PC Card Specification*. Available from www.proxim.com

[14] C. E. Perkins and E. M. Royer, "Ad Hoc On-Demand Distance Vector Routing," in *Proceedings of the 2nd IEEE Workshop on Mobile Computing Systems and Applications*, New Orleans, USA, February 1999.

[15] T. Rautiainen, G. Wölfle, and R. Hoppe, "Verifying Path Loss and Delay Spread Predictions of a 3D Ray Tracing Propagation Model in Urban Environments," in *Proceedings of the 56th IEEE Vehicular Technology Conference (VTC) 2002 - Fall*, Vancouver, Canada, September 2002.

[16] G. Riley, "The Georgia Tech Network Simulator," in *Proceedings of ACM SIGCOMM Workshop on Models, Methods and Tools for Reproducible Network Research (MoMeTools'03)*, Germany, August 2003.

[17] *Specification of the Bluetooth System Ver. 1.1*, Bluetooth SIG, 2001.

[18] I. Stepanov, P. Marron, and K. Rothermel, "Mobility Modeling of Outdoor Scenarios for MANETs," in *Proceedings of the 38th Annual Simulation Symposium (ANSS'38)*, San Diego, USA, April 2005.

[19] *Wireless LAN Medium Access Control (MAC) and Physical Layer (PHY) Specifications*, IEEE Standard 802.11b, 1999.

[20] G. Wölfle, R. Hoppe, and F.M. Landstorfer, "A Fast and Enhanced Ray Optical Propagation Model for Indoor and Urban Scenarios, Based on an Intelligent Preprocessing of the Database", in *Proceedings of the 10th IEEE International Symposium on Personal, Indoor and Mobile Radio Communications (PIMRC)*, Osaka, Japan, September 1999.

[21] X. Wu and A. L. Ananda, "Link Characteristics Estimation For IEEE 802.11 DCF Based WLAN," in *Proceedings of the 29th Annual IEEE Conference on Local Computer Networks (LCN 2004)*, Tampa, Finland, November 2004.